

## The Crystal Structure of $\text{Cr}_8\text{O}_{21}$ Determined from Powder Diffraction Data: Thermal Transformation and Magnetic Properties of a Chromium–Chromate–Tetrachromate

P. NORBY\*

*Department of Chemistry, University of Odense, Denmark*

A. NØRLUND CHRISTENSEN

*Department of Chemistry, University of Aarhus, Denmark*

H. FJELLVÅG

*Department of Chemistry, University of Oslo, Norway*

AND M. NIELSEN

*Department of Physics, Risø National Laboratory, Denmark*

Received October 30, 1990; in revised form May 23, 1991

Thermal decomposition of  $\text{CrO}_3$  was utilized to prepare a powder sample of the chromium oxide usually designated  $\text{Cr}_3\text{O}_8$ . Combined information from powder diffraction data using synchrotron, conventional X-ray, and neutron radiation allowed determination of the structure. The structure is triclinic ( $a = 5.433(1)$ ,  $b = 6.557(1)$ ,  $c = 12.117(2)$  Å,  $\alpha = 106.36(1)$ ,  $\beta = 95.73(1)$  and  $\gamma = 77.96(1)^\circ$ ) and was refined in the space group  $\text{P}\bar{1}$ . The true composition of the compound is  $\text{Cr}_8\text{O}_{21}$ . There are two distinct types of chromium atoms in the structure, which may be designated the oxidation numbers (III) and (VI), respectively. The structure is built from pairs of edge-sharing  $\text{Cr(III)O}_6$  octahedra linked together by  $\text{Cr(VI)O}_4$  tetrahedra to form sheets. The sheets are then linked together by tetrachromate groups ( $\text{Cr(VI)}_4\text{O}_{13}$ ) to form a three-dimensional structure. Thus, the chromium oxide may be described as  $\text{Cr(III)}_2(\text{Cr(VI)O}_4)_2(\text{Cr(VI)}_4\text{O}_{13})$ . The magnetic properties of  $\text{Cr}_8\text{O}_{21}$  were investigated in the temperature range 5 to 300 K. Above 100 K the compound is paramagnetic. Magnetic susceptibility data indicate a transition to antiferromagnetism around 100 K, but only vague indications for additional magnetic reflections were found with neutron powder diffraction. © 1991 Academic Press, Inc.

### Introduction

Chromium oxides, especially “ $\text{Cr}_3\text{O}_8$ ” and  $\text{Cr}_2\text{O}_5$ , have been extensively studied as potential cathode materials for lithium

batteries (1–8). Lithium insertion is possible, both chemically and electrochemically (8, 9). In order to help understanding the mechanisms behind the physical and chemical properties, detailed knowledge of the structures is necessary. However, so far the crystal structures of these chromium oxides

\* To whom correspondence should be addressed.

have not been determined, mainly due to the unavailability of single crystals.

Thermal decomposition of  $\text{CrO}_3$ , in air or under oxygen pressures, results in the formation of a number of chromium oxides (10). A detailed investigation of the decomposition of  $\text{CrO}_3$  was performed by Wilhelmi (11, 12). The starting material,  $\text{CrO}_3$ , is a Cr(VI) compound containing only tetrahedrally coordinated chromium (13). The final thermal decomposition product is  $\text{Cr}_2\text{O}_3$ , which has only trivalent chromium, Cr(III), with octahedral coordination (14). Among the intermediate decomposition products is  $\text{CrO}_2$ , a well-known ferromagnetic material, which contains only octahedrally coordinated Cr(IV) (15). The exact compositions of the various chromium oxides occurring as intermediates between  $\text{CrO}_3$  and  $\text{CrO}_2$  are still a matter of dispute. However, at least four such distinct chromium oxides appear during the thermal transformation of  $\text{CrO}_3$ . Wilhelmi (12) originally proposed the existence of  $\text{Cr}_3\text{O}_8$  and  $\text{Cr}_2\text{O}_5$  formed in air or at moderate oxygen pressure. At higher oxygen pressures a phase with the same composition as  $\text{Cr}_2\text{O}_5$ , but with a different diffraction pattern, is formed and it was denoted  $\text{Cr}_6\text{O}_{15}$ . Another phase formed at high oxygen pressure is  $\text{Cr}_5\text{O}_{12}$ .

The crystal structure has so far only been determined for  $\text{Cr}_5\text{O}_{12}$ , which contains a mixture of tetrahedrally and octahedrally coordinated chromium atoms (16) at a ratio of 3:2. In general the oxygen coordination around chromium atoms is strongly dependent upon their oxidation state (17). Cr(VI) is always found to have tetrahedral oxygen coordination. Cr(V), which is not an oxidation state commonly obtained by direct synthesis, is likewise found to prefer tetrahedral coordination, e.g., in  $\text{Ba}_3(\text{CrO}_4)_2$  and  $\text{K}_3\text{CrO}_4$  (17, 18). Tetravalent chromium may have either tetrahedral or octahedral oxygen coordination (17), as, e.g., found in  $\text{Ba}_2\text{CrO}_4$  and  $\text{CrO}_2$ , respectively (15, 19), while triva-

lent chromium is always found with octahedral oxygen coordination, e.g.,  $\text{Cr}_2\text{O}_3$  and the chromites. The Cr–O bond length depends on the oxidation state and the oxygen coordination of the chromium atom (11). In  $\text{Cr}_5\text{O}_{12}$  the oxidation states (VI) and (III) were assigned to the tetrahedrally and octahedrally coordinated chromium atoms, respectively (16), i.e., the composition may be described as  $\text{Cr(III)}_2\text{Cr(VI)}_3\text{O}_{12}$ .

The feature of having mixed (VI/III) oxidation states for chromium is also found in the structurally related compounds  $M\text{Cr}_3\text{O}_8$ ,  $M = \text{Li, Na, K, Rb, Cs, and Tl}$  (20). The average oxidation state for chromium in these compounds is five, but the structure determination of  $\text{LiCr}_3\text{O}_8$  (20),  $\text{NaCr}_3\text{O}_8$  (21),  $\text{KCr}_3\text{O}_8$  (22), and  $\text{CsCr}_3\text{O}_8$  (23) revealed chromium atoms with tetrahedral and octahedral coordination, giving the composition  $M(\text{I})\text{Cr(III)}(\text{Cr(VI)O}_4)_2$ . The apparent instability of intermediate oxidation states toward disproportionation suggests that all the chromium oxides between  $\text{CrO}_3$  and  $\text{CrO}_2$  in reality are mixed Cr(VI)–Cr(III) compounds. Existing studies of magnetic properties of  $\text{Cr}_2\text{O}_5$  and  $\text{Cr}_3\text{O}_8$  as well as their ESR spectra and XPS data (24, 7) are in favor of a structure involving only Cr(III) and Cr(VI), but they are not conclusive.

This work reports on the structure and properties of “ $\text{Cr}_3\text{O}_8$ ”. As shown by the structure determination, the true composition is  $\text{Cr}_8\text{O}_{21}$ , so in the following “ $\text{Cr}_3\text{O}_8$ ” will be referred to as  $\text{Cr}_8\text{O}_{21}$ . Different unit cells have been proposed (6, 22) for this phase, but so far neither the structure nor a reliable unit cell has been published. In the present study the structure was determined from powder diffraction data by combining information from neutron diffraction and diffraction using conventional X-ray and synchrotron radiation. Direct methods were used, demonstrating the possibilities of using powder diffraction data for determina-

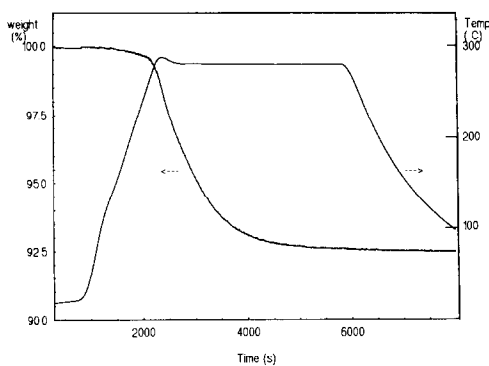


FIG. 1. TG-curve for  $\text{CrO}_3$  heated in air to  $280^\circ\text{C}$ .

tion of even rather complex unknown crystal structures.

### Experimental

The sample of  $\text{Cr}_8\text{O}_{21}$  was prepared by thermal decomposition of  $\text{CrO}_3$  at  $280^\circ\text{C}$  in air; see Ref. (8) for further details. Figure 1 shows a TG curve simulating the synthesis of  $\text{Cr}_8\text{O}_{21}$  by heating  $\text{CrO}_3$  in a mixture of oxygen and nitrogen to  $280^\circ\text{C}$ . The weight loss is approximately 7.0%, giving the composition  $\text{Cr}_8\text{O}_{20.5}$ . The deviation from the ideal composition  $\text{Cr}_8\text{O}_{21}$  may be due to adsorbed water or to a nonstoichiometry in the product. As may be seen from the figure a plateau in the thermal decomposition has been reached. This may be compared to published TG curves for  $\text{CrO}_3$  (e.g., Refs. (11, 12)).

The thermal stability was studied by heating  $\text{Cr}_8\text{O}_{21}$  in an open quartz capillary. An orthorhombic phase appears over the temperature range  $350$  to  $400^\circ\text{C}$ . From powder X-ray diffraction data at room temperature the orthorhombic unit cell dimensions for this phase were found to be  $a = 12.452(2)$ ,  $b = 10.563(2)$ , and  $c = 8.098(2)$  Å. The diffraction pattern is significantly different from those reported for  $\text{Cr}_2\text{O}_5$  and  $\text{Cr}_6\text{O}_{15}$ , but judged from its unit cell dimen-

sions and TG data, the composition of the new phase is close to  $\text{CrO}_{2.5}$ . The work concerning this phase is now in further progress.

Several sets of powder diffraction data were collected during this study using synchrotron, conventional X-ray, and neutron radiation. Synchrotron powder diffraction data were obtained at HASYLAB, Hamburg. The data were collected from  $4.5^\circ$  to  $61.5^\circ$  in  $2\theta$  using a position-sensitive detector covering  $2.7^\circ$  in  $2\theta$  at a wavelength of  $1.2990$  Å; for further experimental details, see Ref. (25). Neutron powder diffraction data were collected from  $6^\circ$  to  $159^\circ$  in  $2\theta$  with a step length  $0.05^\circ$  in  $2\theta$ , using the DIA instrument at ILL, Grenoble. The wavelength was  $1.9589$  Å. X-ray powder diffraction data were collected at the Institut für Kristallographie und Petrographie, ETH, Zürich, at a Scintag PAD-X diffractometer equipped with a solid state detector and using  $\text{CuK}\beta$  radiation ( $\lambda = 1.39222$  Å). The fluorescence from chromium was efficiently removed by energy discrimination. The data were collected from  $5^\circ$  to  $90^\circ$  in  $2\theta$  using a step length of  $0.02^\circ$ . Low temperature powder neutron diffraction data were collected at  $20$  K with the OPUS III two-axis diffractometer at JEEP II, Kjeller, Norway, using a Displex cooling system. For phase identification and unit cell refinement Guinier data were collected using  $\text{CrK}\alpha_1$  radiation ( $\lambda = 2.289753$  Å) in order to reduce problems due to fluorescence.

The trial-and-error indexing program TREOR (26) was used in the attempts of determining the unit cell and the CELLKANT program (27) was used to refine the unit cell from observed  $d$ -spacings. Structure factors were extracted from the powder diagrams with the deconvolution program ALLHKL (28). The extracted structure factors were used in direct methods calculations using the programs MULTAN77 (29) and XTAL (30). Difference Fourier calculations were performed with the program sys-

tem XRS-82 (31), and crystal structure refinements were carried out using the programs XRS-82 and EDINP (32).

High temperature powder X-ray diffraction data for temperatures up to 600°C were measured using a Guinier Simon camera ( $\text{CuK}\alpha_1$  radiation) with the temperature change being synchronized with the movement of the film cassette. Fluorescence from chromium was diminished by using a Ni-foil in front of the photographic film.

Thermogravimetric measurements were performed using a SETARAM TG 92-12 instrument. Magnetic susceptibility data were collected between 5 and 300 K using a SQUID magnetometer (MPMS, Quantum Design) and magnetic fields 100–1000 Oe.

## Results and Discussion

### Structure Determination

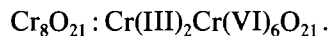
The first step required in the process of solving the crystal structure of  $\text{Cr}_8\text{O}_{21}$  was to determine the correct unit cell. The X-ray diffraction pattern of the synthesized chromium oxide matched the published patterns of the chromium oxide usually referred to as  $\text{Cr}_3\text{O}_8$ . However, a successful indexing of the powder pattern obtained from microdensitometer readings of the Guinier films proved impossible. The solution of the indexing problem was provided by synchrotron data, where the resolution of the diffraction peaks is considerably improved, although possibly here being limited by the degree of crystallinity of the sample. The synchrotron powder X-ray diffractogram of  $\text{Cr}_8\text{O}_{21}$  was completely indexed with a triclinic unit cell using the TREOR program (25) with a figure of merit,  $M_{20}$ , of 30.3. The refined unit cell dimensions ( $\text{CrK}\alpha_1$ -Guinier data) are

$$a = 5.433(1), b = 6.557(1), c = 12.117(2) \text{ \AA}, \\ \alpha = 106.36(1), \beta = 95.73(1), \text{ and} \\ \gamma = 77.96(1)^\circ;$$

the indexed powder diagram is provided in Table I. The number of observed reflections is considerably less than calculated from the triclinic unit cell. However, when calculating the intensities of the reflections based on the refined structural model, the reflections not observed are generally of very low intensity. Furthermore, in the high  $2\theta$  range there is a high degree of overlapping reflections, making separation of weak reflections difficult.

This unit cell is consistent with published electron diffraction patterns (6) of  $\text{Cr}_3\text{O}_8$ . From the original diffraction picture, kindly donated by Professor Y. Takeda, two axes of 5.5 and 6.6 Å at an angle of 102° could be recognized, thereby matching the  $a$ ,  $b$ , and  $\gamma$  of the here found triclinic unit cell. The crystals used in the electron diffraction study were platelike, with  $a$  and  $b$  in the plane, indicating a layer like structure.

The volume of the unit cell does not fit with an integral number of  $\text{Cr}_3\text{O}_8$  formula units when the observed density (3.0 g/cm<sup>3</sup>) is considered. The expected unit cell volume per chromium atom is  $\sim 50 \text{ \AA}^3$ , as derived by interpolation using values observed for other chromium oxides. Expecting the oxidation states of the chromium atoms to be restricted to III and VI, a possible composition of the chromium oxide (with one chromium atom per  $50.4 \text{ \AA}^3$ ) would be



The uneven number of oxygen atoms means that if the structure is centrosymmetric one of the oxygen atoms must be situated at a center of symmetry.

The second step in the determination of the unknown  $\text{Cr}_8\text{O}_{21}$  structure directly from powder diffraction data was the extraction of reliable individual structure factors from the powder diagram. The data were thereafter treated as a single crystal data set and conventional direct methods programs were applied. The low symmetry of the structure is actually an advantage since the structure

TABLE I

INDEXED X-RAY POWDER DIFFRACTION PATTERN  
FOR Cr<sub>8</sub>O<sub>21</sub>

<i>h</i>	<i>k</i>	<i>l</i>	<i>d</i> <sub>calc</sub>	<i>d</i> <sub>obs</sub>	Intensity
0	0	1	11.62	11.66	95
0	-1	1	6.185	6.192	20
0	1	0	6.178		
0	0	2	5.807	5.809	20
0	-1	2	4.944		
0	1	1	4.934	4.938	20
1	0	1	4.750	4.755	5
1	1	0	4.465	4.470	25
-1	-1	2	4.015		
-1	0	2	4.007	4.007	10
1	1	1	3.879	3.879	40
0	0	3	3.872		
1	0	2	3.836	3.837	75
0	-1	3	3.766		
0	1	2	3.758	3.758	25
1	-1	0	3.696	3.699	50
-1	1	1	3.397	3.399	25
-1	-1	3	3.330		
1	-1	2	3.320	3.323	100
0	-2	1	3.206		
1	1	2	3.201	3.201	45
-1	0	3	3.195		
0	-2	2	3.093	3.091	65
0	2	0	3.089		
1	0	3	3.065	3.067	35
-1	-2	1	3.039	3.041	25
0	-1	4	2.950	2.951	20
-1	1	2	2.949		
0	0	4	2.904	2.906	2
1	-1	3	2.866	2.867	5
0	-2	3	2.810	2.811	30
-1	-2	3	2.723	2.717	2
2	0	0	2.654	2.657	35
-2	-1	1	2.652		
2	1	0	2.626	2.626	65
-2	0	1	2.613	2.615	20
-1	0	4	2.596	2.596	25
-1	1	3	2.515	2.515	2
1	0	4	2.502	2.503	5
2	1	1	2.478	2.479	5
1	-1	4	2.443	2.444	10
0	-1	5	2.396	2.395	5
0	1	4	2.393		
2	0	2	2.375	2.375	5

Note: Guinier, CrK $\alpha_1$  radiation,  $\lambda = 2.289753$  Å indexing based on a triclinic unit cell:

$a = 5.433(1)$ ,  $b = 6.557(1)$ ,  $c = 12.117(2)$  Å

$\alpha = 106.36(1)$ ,  $\beta = 95.73(1)$ ,  $\gamma = 77.96(1)^\circ$

Unit cell volume = 404.7 Å<sup>3</sup>.

TABLE I—Continued

1	2	2	2.360	2.360	2
0	0	5	2.323	2.323	5
1	-2	3	2.297	2.297	5
-2	-2	2	2.266	2.266	5
-2	0	3	2.235	2.235	5
2	2	0	2.233		
2	-1	2	2.174	2.171	5
-1	0	5	2.163		
-2	-2	3	2.162	2.162	10
2	0	3	2.146	2.147	10
-1	2	2	2.132		
-1	-3	1	2.131	2.131	35
0	-3	2	2.129		
1	-2	4	2.095	2.096	2
1	0	5	2.095		
-2	1	2	2.085	2.085	5
-1	-3	3	2.077	2.077	10
0	3	0	2.059	2.059	5
2	1	3	2.030	2.030	5
0	1	5	2.005	2.005	15
-2	0	4	2.003		
0	0	6	1.9358	1.9373	10
-2	-1	5	1.8938	1.8935	10
-2	-3	2	1.8644	1.8641	5
-2	-3	1	1.8547	1.8560	5
2	-2	0	1.8480	1.8482	20
-2	-2	5	1.8349	1.8337	5
1	2	4	1.8218	1.8212	5
-1	3	0	1.8082	1.8092	5
1	-3	3	1.7973	1.7961	10
-2	0	5	1.7873	1.7875	5
3	0	0	1.7696	1.7683	10
-3	0	1	1.7610	1.7603	5
-2	-3	4	1.7511	1.7517	2
3	1	1	1.7405	1.7393	5
-1	3	1	1.7296	1.7301	5
2	3	1	1.7119		
2	0	5	1.7113	1.7112	30
-3	-2	2	1.6995	1.6998	5
-2	-1	6	1.6902	1.6907	10
3	0	2	1.6725	1.6736	5
-1	-3	6	1.6654	1.6658	5
-2	-2	6	1.6649		
0	0	7	1.6592		
0	-2	7	1.6588	1.6583	20
0	2	5	1.6555	1.6545	5
1	3	3	1.6331	1.6326	5
-1	1	6	1.6300	1.6294	2
3	-1	1	1.6131		
1	2	5	1.6129	1.6130	2
2	3	2	1.6039		
-1	0	7	1.6038	1.6042	2

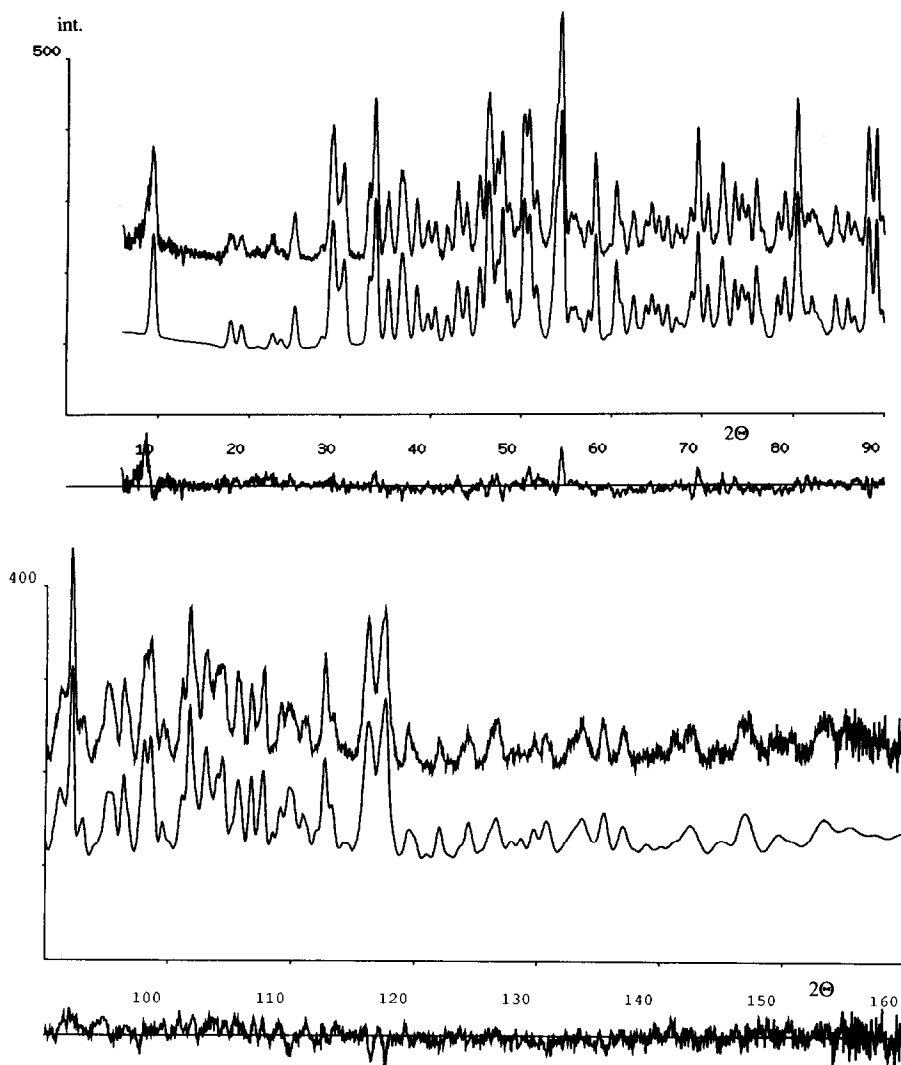


FIG. 2. Observed, calculated, and difference powder neutron diffraction profiles.

determination demands a large number of unique reflections. On the other hand, the amount of information is clearly limited due to overlapping reflections, in particular at higher scattering angles.

A reasonable strategy is to determine the chromium positions from X-ray data, since oxygen has a relatively low scattering power. Once having determined the chromium coordinates, oxygen atoms may be

revealed using difference Fourier calculations. However, a definite determination of their coordinates should imply neutron diffraction refinements, since oxygen compared to chromium has a larger scattering length for neutrons.

The statistics of the synchrotron diagram were unfortunately too poor to allow determination of the structure. Nor was this possible on the basis of the high resolution neu-

tron diffraction data. However, it proved possible to solve the structure using the X-ray powder diffraction data (ETH, Zürich).

Individual structure factors for the reflections were extracted from the X-ray powder diffractogram by deconvolution, using the ALLHKL program (27). A set of 315 structure factors were used in the subsequent determination of the structure by direct methods. The only possible space groups are  $P\bar{1}$  and  $P1$ . However, attempts to solve the structure in the centrosymmetric space group were not successful, but for the space group  $P1$  a large part of the structure was located. The obtained structure was, however, very close to being centrosymmetric and it was therefore transformed into the centrosymmetric space group  $P\bar{1}$ , thereby reducing the number of free positional parameters. Direct methods (in  $P1$ ) provided all the chromium atoms as the 8 highest peaks in the electron density map, which transform into four twofold positions in  $P\bar{1}$ . By considering plausible bond distances, 15 oxygen atoms could be identified among the next 20 peaks in the electron density map. When transformed into  $P\bar{1}$  this gives eight twofold oxygen positions. Thus in the asymmetric unit 4 chromium atoms and 8 oxygen atoms were obtained using direct methods. Two additional oxygen atoms were located by difference Fourier calculations using the powder neutron diffraction data. By considering the Cr–Cr distances in the derived structure and the oxygen coordination around the chromium atoms, it was obvious that one oxygen atom was still missing in the structure. Difference Fourier calculations failed to reveal this oxygen. The only plausible position for the last oxygen atom was on a center of symmetry, linking two CrO<sub>4</sub> tetrahedra and giving a total of 21 oxygens in the unit cell.

An oxygen atom situated at a center of

TABLE II  
FINAL PARAMETERS FROM THE REFINEMENT  
OF Cr<sub>8</sub>O<sub>21</sub>.

Atom	x	y	z	B(Å <sup>2</sup> )
CR1	0.859(3)	0.211(2)	0.068(1)	1.5
CR2	0.280(2)	0.234(2)	0.898(1)	1.7
CR3	0.358(2)	0.377(2)	0.258(1)	2.1
CR4	0.721(3)	0.799(2)	0.528(1)	3.2
O1	0.800(1)	0.504(1)	0.060(1)	1.5
O2	0.426(1)	0.835(1)	0.049(1)	1.5
O3	0.5	0.0	0.5	8.6
O4	0.127(2)	0.250(1)	0.182(1)	1.4
O5	0.381(1)	0.727(1)	0.812(1)	1.6
O6	0.696(1)	0.859(1)	0.243(1)	2.6
O7	0.911(1)	0.899(1)	0.057(1)	0.6
O8	0.383(2)	0.358(1)	0.397(1)	2.2
O9	0.038(2)	0.115(2)	0.406(1)	7.5
O10	0.183(2)	0.372(1)	0.591(1)	3.4
O11	0.261(2)	0.632(1)	0.255(1)	3.4
No. of contributing reflections:			914	
R-factors(%): $R_F$			5.7	
			$R_1$	11.5
			$R_P$	4.8
			$R_{wp}$	6.3

Note. Standard deviations in parentheses.

symmetry must necessarily have a 180° Cr–O–Cr bond. This is an energetically rather unfavorable arrangement, and in the linkage of two CrO<sub>4</sub> tetrahedra this is not likely to occur. This indicates that the structure either is not truly centrosymmetric or that static or dynamic disorder occurs.

The final refinements of the structure (in  $P\bar{1}$ ), based on the neutron diffraction data, were performed using the EDINP refinement program (31). In Fig. 2 the observed, calculated, and difference profiles after the final refinement are shown. The structural parameters and  $R$ -values are given in Table II, and the interatomic distances and angles are listed in Table III. Refinement of the population parameters of the oxygen atoms gave occupancies between 0.99 and 1.07, with all coordinates being stable, and only

TABLE III  
INTERATOMIC DISTANCES(Å) AND ANGLES(°) IN Cr<sub>8</sub>O<sub>21</sub>

Cr1-O1	1.91(2)	Cr1-O2	2.01(2)
O4	1.91(2)	O5	1.95(2)
O7	1.98(2)	O7'	1.94(2)
Mean Cr1-O: 1.95			
O1-Cr1-O2	87.7(7)	O1-Cr1-O4	93.6(7)
O1 O5	93.6(6)	O1 O7	173.3(9)
O1 O7'	95.2(8)	O2 O4	178.2(10)
O2 O5	88.4(7)	O2 O7	86.9(6)
O2 O7'	88.3(6)	O4 O5	90.3(7)
O4 O7	91.8(7)	O4 O7'	92.7(7)
O5 O7	90.2(8)	O5 O7'	170.5(6)
O7 O7'	80.7(6)		
Cr2-O1	1.62(1)	Cr2-O2	1.68(1)
O6	1.65(1)	O7	1.70(2)
Mean Cr2-O: 1.66			
O1-Cr2-O2	107.7(8)	O1-Cr2-O6	112.7(9)
O1 O7	114.0(8)	O2 O6	104.0(7)
O2 O7	108.3(8)	O6 O7	109.6(8)
Cr3-O4	1.70(2)	Cr3-O5	1.64(1)
O8	1.72(2)	O11	1.65(2)
Mean Cr3-O: 1.68			
O4-Cr3-O5	108.0(7)	O4-Cr3-O8	110.2(9)
O4 O11	104.1(8)	O5 O8	110.5(8)
O5 O11	110.5(10)	O8 O11	110.1(7)
Cr4-O3	1.67(1)	Cr4-O8	1.76(2)
O9	1.59(2)	O10	1.61(1)
Mean Cr4-O: 1.66			
O3-Cr4-O8	114.8(9)	O3-Cr4-O9	111.9(10)
O3 O10	109.9(9)	O8 O9	109.0(10)
O8 O10	104.2(9)	O9 O10	106.5(10)
Cr1-O1-Cr2	158.6(8)	Cr1-O2-Cr2	153.0(6)
Cr4-O3-Cr4'	180	Cr1 O4 Cr3	154.3(9)
Cr1-O5-Cr3	158.6(8)	Cr3 O8 Cr4	136.3(8)
Cr1-O7-Cr1'	99.3(7)	} Mean: 118.6	
Cr1-O7-Cr2	127.9(7)		
Cr1'-O7-Cr2	128.6(7)		

a slight reduction in the *R*-values. In order to further verify that the obtained structure was correct, the model was tested using the X-ray data set. The refinement converged with atomic positions very close to those obtained from the neutron data set. Due to peak asymmetry and probably preferred orientation in the sample, the fit was not per-

fect. However, the agreement between the observed and the calculated X-ray pattern, shown in Fig. 3, is convincing.

#### Structure Description

The structure of Cr<sub>8</sub>O<sub>21</sub> contains two CrO<sub>6</sub> octahedra sharing one edge. Two (symmetry related) chromate groups (CrO<sub>4</sub> tetrahe-



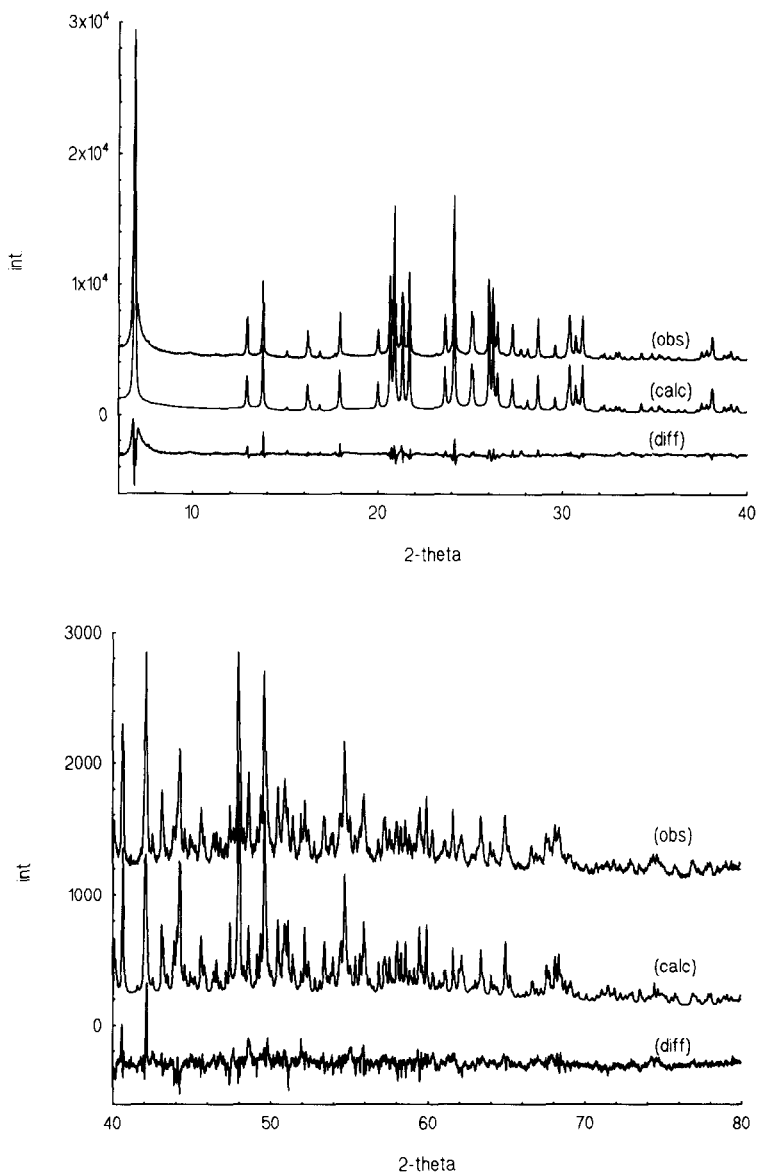


FIG. 3. Observed, calculated, and difference powder X-ray diffraction profiles.

dra) are linking the double octahedra together to form a sheet. These sheets are finally linked together by tetrachromate groups ( $\text{Cr}_4\text{O}_{13}$ ) to form a three-dimensional framework. A polyhedra representation of the structure is shown in Fig. 4. Structural details of the atomic arrangement around

the double octahedra and the tetrachromate group are shown in Fig. 5. A number of interesting coordination features should be noticed. The oxygens linking the two octahedra together are each bonded to three chromium atoms, see Fig. 5a. The Cr2-chromate groups are linked to three  $\text{CrO}_6$  octahe-

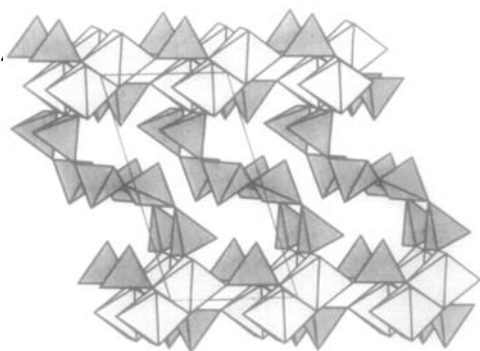


FIG. 4. A polyhedra representation of the structure of  $\text{Cr}_8\text{O}_{21}$  viewed along the  $a$ -axis.

dra and thus have one terminated oxygen bond. Figure 5b shows the tetrachromate group in detail. The tetrachromate group has a center of symmetry (O3). The "terminal" chromium atoms (Cr3) are coordinated by two oxygen atoms of the octahedra, by one oxygen from the neighboring "inner" Cr4-chromate group, and by one terminating oxygen atom. Cr4 is linked only to chromate groups (Cr3 and symmetry related Cr4) and has therefore two terminating oxygen atoms in the coordination shell. The oxygen atom at the center of the tetrachromate group is linking the two Cr4 atoms and is situated at a center of symmetry.

#### Discussion of Structural Features

Two types of coordination are found for chromium atoms in  $\text{Cr}_8\text{O}_{21}$ . For the octahedrally coordinated atoms the mean Cr–O bond distance is 1.95 Å, see Table III. This agrees well with Cr–O distances commonly found in Cr(III) oxides, and it is thus reasonable to assign oxidation state (III) to the octahedrally coordinated chromium atom. The nonequivalent tetrahedrally coordinated chromium atoms in the asymmetric unit have mean Cr–O distances varying between 1.66 and 1.68 Å, which is compatible with an oxidation state of (VI) for chromium. The oxidation states are in agreement

with the stoichiometry found and  $\text{Cr}_8\text{O}_{21}$  is thus a chromium–chromate–tetrachromate,  $\text{Cr(III)}_2(\text{Cr(VI)}\text{O}_4)_2\text{Cr(VI)}_4\text{O}_{13}$ .

As observed in other chromium oxides (11), like  $\text{CrO}_3$  and  $\text{Cr}_5\text{O}_{12}$ , terminating Cr–O bonds are generally shorter than the bonds between chromium and bridging oxygen atoms (Cr–O–Cr). This is also found in the structure of  $\text{Cr}_8\text{O}_{21}$ , most visible in the coordination around Cr4 for the distances Cr4–O9 and Cr4–O10. The other terminating Cr–O distances (Cr2–O6 and Cr3–O11) are not distinctly different from the bridging ones, which, however, may be an artifact brought out by the relatively low accuracy in the structure determination based on the present powder diffraction data.

Singly coordinated oxygen atoms are expected to have larger thermal vibrational ellipsoids than two- and three-coordinated oxygen atoms. Indeed Table II shows that the temperature factors for O6, O9, O10, and O11 are the largest ones, while the three-coordinated oxygen atom (O7) has a small temperature factor. The temperature factor of the oxygen atom situated at a center of symmetry (O3) is large, indicating the existence of static or dynamic disorder for this oxygen atom caused by the energetically unfavorable  $180^\circ$  Cr–O–Cr angle. In  $\text{Rb}_2\text{Cr}_4\text{O}_{13}$  the Cr–O–Cr angles in the tetrachromate group are 120.5, 139.3, and  $147.2^\circ$ , respectively (33), which are close to the value of the Cr3–O8–Cr4 angle in  $\text{Cr}_8\text{O}_{21}$  ( $136^\circ$ ). Probably a better description of O3 and the tetrachromate group could be achieved in the space group  $P1$ ; however, the already large numbers of parameters in the refinement do not allow such a reduction of symmetry with the present data sets. The temperature factors for the chromium atoms are smallest for the atoms in the layer (Cr1 and Cr2), whereas in the tetrachromate group they have a larger thermal motion. The absolute values of the temperature factors should not be taken

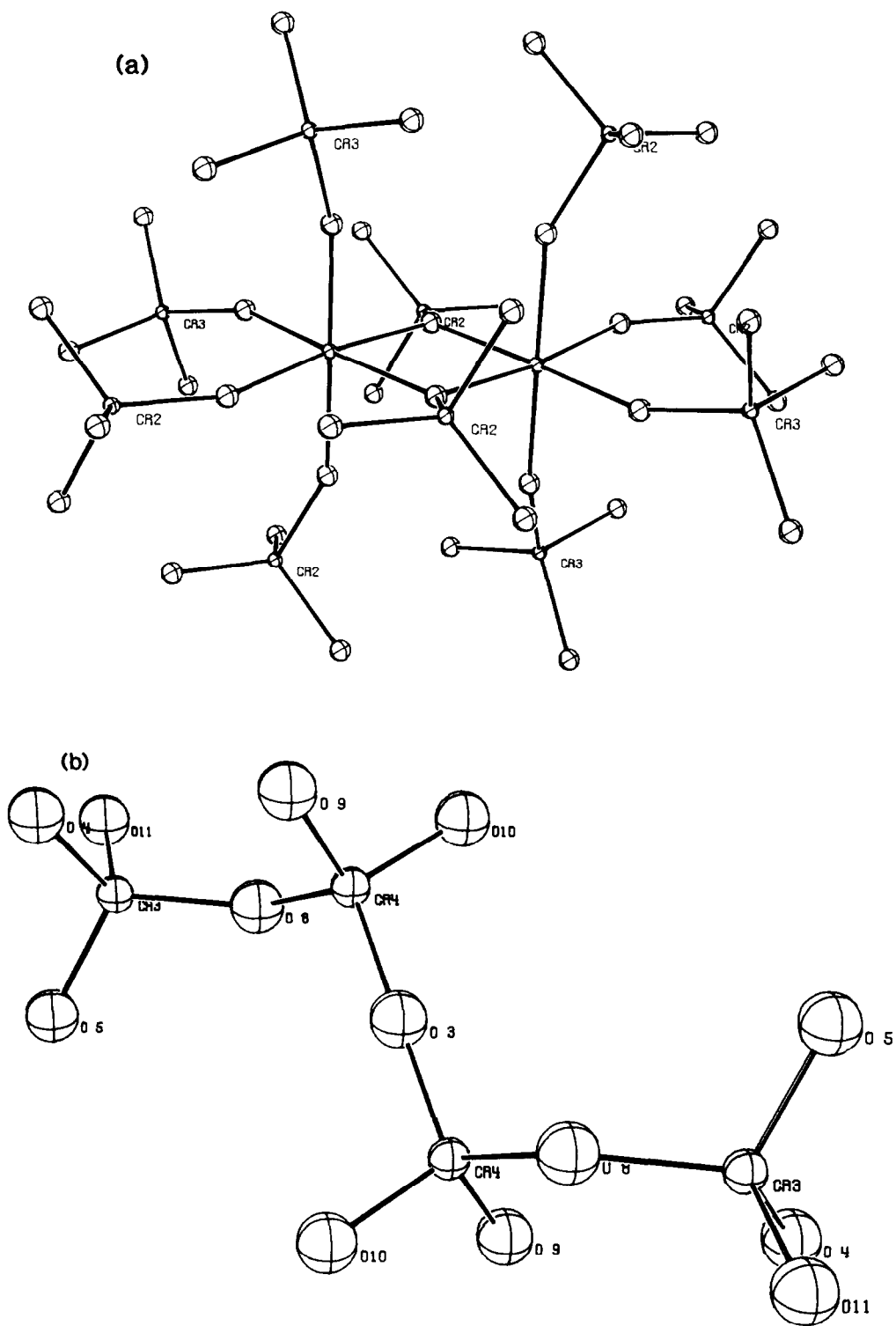


FIG. 5. Details from the structure of  $\text{Cr}_8\text{O}_{21}$ . (a) The double-octahedron. (b) The tetrachromate group.

literally since they are strongly dependent on, e.g., the chosen background function in the powder diffraction diagram.

The structure of  $\text{Cr}_8\text{O}_{21}$  has features in common with, e.g.,  $\text{Cr}_5\text{O}_{12}$  (16) and  $\text{CrO}_3$  (13). An arrangement with pairs of edgesharing Cr(III) octahedra linked by chromate groups to form sheets is also found in  $\text{Cr}_5\text{O}_{12}$ , which is the only other structurally characterized chromium oxide of composition intermediate between  $\text{CrO}_3$  and  $\text{CrO}_2$ . Although the linkage of the edgesharing double octahedra in  $\text{Cr}_5\text{O}_{12}$  is different from that in  $\text{Cr}_8\text{O}_{21}$ , the oxygen atom linking the two octahedra is in both cases three-coordinated. The sheet formed by the double octahedra and the single chromate groups may for both oxides be designated as  $[\text{Cr}_2(\text{CrO}_4)_2]_n^{2n+}$ . In  $\text{Cr}_5\text{O}_{12}$  the anions linking the sheets are chromate groups, thus forming a rather dense three-dimensional structure. In  $\text{Cr}_8\text{O}_{21}$  the layers are linked by tetrachromate groups resulting in a somewhat less dense structure having a larger interlayer distance. Thus, the (yet unknown) structures of  $\text{Cr}_2\text{O}_5$  ( $\text{Cr}_6\text{O}_{15}$ ) may possibly be composed of sheets of composition  $\text{Cr}_2(\text{CrO}_4)_2$ , but linked together by dichromate groups. The structure of  $\text{CrO}_3$  is one-dimensional and composed entirely of chains of  $\text{CrO}_4$  tetrahedra held together only by Van der Waal forces. All Cr(VI) atoms in  $\text{CrO}_3$  therefore have two neighboring oxygen atoms, which are singly coordinated and two oxygen atoms linking the chromium atoms. The central atoms in the tetrachromate group in  $\text{Cr}_8\text{O}_{21}$  have similar oxygen surroundings, and one may consider the formation of longer polychromates for the more oxygen rich chromium oxides to have reached the limit of infinity in the structure of  $\text{CrO}_3$ .

#### Magnetic Properties of $\text{Cr}_8\text{O}_{21}$

The crystal structure of  $\text{Cr}_8\text{O}_{21}$  contains two distinct types of chromium atoms.

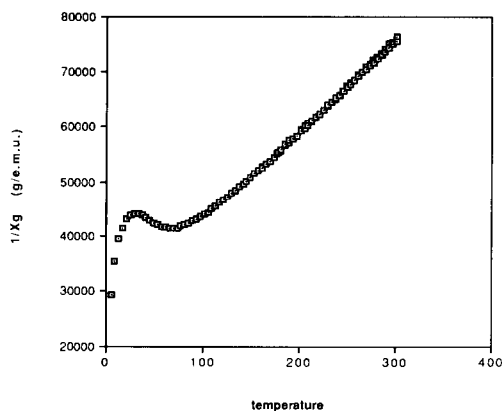


FIG. 6. Inverse susceptibility of  $\text{Cr}_8\text{O}_{21}$  versus temperature.

Based on interatomic distances and coordination polyhedra the description of the compound as  $\text{Cr(III)}_2\text{Cr(VI)}_6\text{O}_{21}$  seems plausible. The present study of the magnetic properties of  $\text{Cr}_8\text{O}_{21}$  differs only slightly from that of Hewston and Chamberlain (24) for the compound they designated as  $\text{Cr(III)}_2\text{Cr(VI)}_7\text{O}_{21}$ . Earlier reported EPR spectra of a similar chromium oxide give conclusive evidence for the existence of the Cr(III) oxidation state (7).

In accordance with the presence of Cr(III) atoms,  $\text{Cr}_8\text{O}_{21}$  is paramagnetic at room temperature. The inverse susceptibility versus temperature curve (Fig. 6) obeys the Curie-Weiss law over the temperature range 100–300 K. From this section of the  $\chi^{-1}(T)$  curve, an effective paramagnetic moment  $\mu_p = 4.2(1) \mu_B$  and a  $\theta$  value of  $-164(5)$  K are calculated. The paramagnetic moment exceeds somewhat the expected spin-only value for a  $d^3$  ion ( $\mu_p = 3.87 \mu_B$ ). However, this observation complies with the findings for, e.g.,  $\text{KCr}_3\text{O}_8$  [ $4.1\text{--}4.2 \mu_B$  per Cr(III)] and  $\text{Cr}_2\text{O}_3$  [ $4.2\text{--}4.3 \mu_B$  per Cr(III)].

The low temperature part of the  $\chi^{-1}(T)$  curve clearly indicates the existence of long range antiferromagnetic order. The  $\chi^{-1}(T)$  curve deviates from the Curie-Weiss behavior for  $T < 100$  K. Neutron powder dif-

fraction carried out at temperatures between 10 and 100 K showed only a few very weak additional magnetic reflections. However, because of the very low intensity their temperature dependence could not be used for an accurate determination of  $T_N$ , nor could the magnetic structure be solved on the basis of the sparse data.

### Acknowledgments

Dr. M. S. Lehmann, ILL, Grenoble, is thanked for helping with the room temperature neutron diffraction measurements and for very valuable discussions. René Koksang, ERL, Denmark, is thanked for preparation of the Cr<sub>8</sub>O<sub>21</sub> sample used in this investigation. The use of the powder diffractometer at the Institut für Kristallographie und Petrographie, ETH, Zürich, was kindly made possible by Dr. Christian Baerlocher. For the donation of the electron diffraction pictures Professor Y. Takeda, Japan, is thanked. Dr. A. F. Andresen is thanked for help in the powder diffraction experiments at Kjeller, Norway.

### References

1. J. O. BESENHARD AND R. SHOLLHORN, *J. Electrochem. Soc.* **124**, 968 (1977).
2. J. O. BESENHARD, J. HEYDECKE, AND H. P. FRITZ, *Solid State Ionics* **6**, 215 (1982).
3. J. O. BESENHARD, J. HEYDECKE, E. WUDY, AND H. P. FRITZ, *Solid State Ionics* **8**, 61 (1983).
4. Y. TAKEDA, R. KANNO, Y. TSUJI, O. YAMAMOTO, AND H. TAGUSH, *J. Power Sources* **9**, 325 (1983).
5. Y. TAKEDA, R. KANNO, Y. TSUJI, AND O. YAMAMOTO, *J. Electrochem. Soc.* **131**, 2006 (1984).
6. Y. TAKEDA, R. KANNO, Y. OYABE, AND O. YAMAMOTO, *J. Power Sources* **14**, 215 (1985).
7. O. YAMAMOTO, Y. TAKEDA, R. KANNO, Y. OYABE, AND Y. SHINYA, *J. Power Sources* **20**, 151 (1987).
8. R. KOKSBANG AND P. NORBY, *Electrochim. Acta* **36**, 727 (1991).
9. P. NORBY, R. KOKSBANG, AND H. FJELLVÅG, to be published.
10. R. S. SCHWARTZ, I. FANKUCHEN, AND R. WARD, *J. Amer. Chem. Soc.* **74**, 1676 (1952).
11. K. A. WILHELMI, Ph.D. thesis, University of Stockholm, Sweden, 1966.
12. K. A. WILHELMI, *Acta Chem. Scand.* **22**, 2565 (1968).
13. J. S. STEPHENS AND D. W. J. CRUICKSHANK, *Acta Crystallogr. Sect. B* **26**, 222 (1970).
14. R. E. NEWNHAM AND Y. M. DE HAAN, *Z. Kristallogr.* **117**, 235 (1962).
15. A. MICHEL AND J. BÉNARD, *Compt. Rend.* **200**, 1016 (1935).
16. K. A. WILHELMI, *Acta Chem. Scand.* **19**, 165 (1965).
17. A. F. WELLS, "Structural Inorganic Chemistry," Clarendon Press, Oxford 1975.
18. H. MATTAUSCH AND H. MÜLLER-BUSCHBAUM, *Z. Naturforsch* **10**, 27 (1972).
19. H. MATTAUSCH AND H. MÜLLER-BUSCHBAUM, *Z. Anorg. Chem.* **407**, 129 (1974).
20. K. A. WILHELMI, *Arkiv Kemi.* **26**, 131 (1966).
21. P. NORBY, H. FJELLVÅG, AND R. KOKSBANG, in preparation.
22. K. A. WILHELMI, *Acta Chem. Scand.* **12**, 1965 (1958).
23. K. A. WILHELMI, *Arkiv Kemi.* **26**, 141 (1966).
24. T. A. HEWSTON AND B. L. CHAMBERLAND, *J. Magn. Magn. Mater.* **43**, 89 (1984).
25. M. S. LEHMANN, A. NØRLUND CHRISTENSEN, H. FJELLVÅG, R. FEIDENHANS'L, AND M. NIELSEN, *J. Appl. Crystallogr.* **20**, 123 (1987).
26. P.-E. WERNER, L. ERIKSSON, AND M. WESTDAHL, *J. Appl. Crystallogr.* **18**, 367 (1985).
27. N. O. ERSSON, "Program CELLKANT," Chemical Institute, Uppsala University, Uppsala, Sweden 1981.
28. G. S. PAWLEY, *J. Appl. Crystallogr.* **18**, 367 (1985).
29. P. MAIN, L. LESSINGER, M. M. WOOLFSON, G. GERMAIN, AND J.-P. DECLERCQ, "MULTAN," Universities of York, England, and Louvain, Belgium (1977).
30. J. M. STEWART AND S. R. HALL, "XTAL Structure Determination System," Tech. Rep. TR-1364. Computer Science Center, Univ. of Maryland, College Park, Maryland.
31. CH. BAERLOCHER, "The XRS-82 System," Inst. für Krist. & Petrogr., ETH, Zürich, 1982.
32. G. S. PAWLEY, *J. Appl. Crystallogr.* **13**, 630 (1980).
33. P. LÖFGREN, *Acta. Crystallogr. Sect. B* **29**, 2141 (1973).